Bioorganic Chemistry 84 (2019) 186–191

Contents lists available at ScienceDirect

Bioorganic Chemistry

journal homepage: www.elsevier.com/locate/bioorg

Antitrypanosomal activity of *epi*-polygodial from *Drimys brasiliensis* and its effects in cellular membrane models at the air-water interface

Giulia Elisa Guimarães Gonçalves[a], Thiago Rahal Morais[a], Kaio de Souza Gomes[b], Thais Alves Costa-Silva[b], Andre Gustavo Tempone[c], João Henrique Ghilardi Lago[b], Luciano Caseli[a,*]

[a] Instituto de Ciências Ambientais, Químicas e Farmacêuticas, Universidade Federal de São Paulo, São Paulo, Brazil
[b] Centro de Ciências Naturais e Humanas, Universidade Federal do ABC, Santo André, Brazil
[c] Centro de Parasitologia e Micologia, Instituto Adolfo Lutz, São Paulo, Brazil

ARTICLE INFO

Keywords:
Epi-polygodial
Trypanosoma cruzi
Langmuir monolayers
Air-water interface

ABSTRACT

Epi-polygodial, a drimane sesquiterpene was isolated from *Drimys brasiliensis* (Winteraceae). This compound demonstrated high parasite selectivity towards *Trypanosoma cruzi* trypomastigotes (IC_{50} = 5.01 μM) with a selectivity index higher than 40. These results were correlated with the effects observed when this compound was incorporated in cellular membrane models of protozoans, represented by Langmuir monolayers of dipalmitoylphosphoethanolamine (DPPE). Surface pressure-area isotherms showed that *epi*-polygodial expands DPPE monolayers at higher areas and condenses them at lower areas, which was attributed to the preferential interaction with the polar heads of the lipid. This mechanism of action could be corroborated with Polarization-Modulation Reflection-Absorption Spectroscopy and Brewster Angle Microscopy. These results pointed to the fact that the interaction of *epi*-polygodial with DPPE monolayers at the air-water interface affects the physical chemical properties of the mixed film, which may be important to comprehend the interaction of this drug with cellular membranes at the molecular level.

1. Introduction

Polygodial is a drimane skeleton sesquiterpene found in several plant species from *Polygonum* and *Drimys*. This compound exhibited fungicide [1], anti-inflammatory [2] and anti-leishmanial [3] activities. Although similar to polygodial, the occurrence of its C-9 isomer, *epi*-polygodial, has previously been detected exclusively in *Drimys winterri* [4].

The effect of polygodial against *Trypanosoma cruzi*, specifically to trypomastigote forms, has previously been reported by our group [3]. Effects against *Trypanosoma cruzi* are frequently associated to intracellular amastigotes since this form is considered the most relevant stage of the parasite [5]. However, the discovery of active compounds against trypomastigotes (extracellular forms) could be important, especially in studies aiming the determination of mechanisms of action of bioactive compounds. These facts are relevant to investigative the biological activity of *epi*-polygodial and to correlate with models of biological systems. One of these models is the Langmuir films, which are monolayers of insoluble amphiphiles formed at liquid-gas interfaces [6]. Monolayers formed from membrane lipids at the air-water interface can set up a model for half a membrane [7], and have been employed in the last decades to investigate interactions of bioactive compounds with cellular membranes at the molecular level [8–10]. With these ideas in mind, in this paper, we investigated the action of *epi*-polygodial in cell membrane models formed of selected lipids at the air-water interface. Particularly, we chose 1,2-dipalmitoyl-sn-glycero-3-phosphoethanolamine (DPPE) since lipids with ethanolamine groups are frequently found in cellular membranes of protozoa [11] and employed as simple model when using Langmuir monolayers [12,13].

2. Materials and methods

2.1. General

NMR spectra were recorded on a spectrometer Varian INOVA-500, operating at 500 (^{1}H) and 125 (^{13}C) MHz, using $CDCl_3$ (Aldrich) as solvent and TMS as the internal standard. LREIMS spectra were recorded on a MS-QP-5050A (70 eV) mass spectrometer. Column

* Corresponding author.
E-mail address: lcaseli@unifesp.br (L. Caseli).

https://doi.org/10.1016/j.bioorg.2018.11.048
Received 23 October 2018; Received in revised form 22 November 2018; Accepted 24 November 2018
Available online 24 November 2018

chromatographic separation procedures were performed using silica gel 60 (230–400 mesh, Merck) for column and silica gel 60 PF254 (Merck) for analytical TLC (0.25 mm). The phospholipid DPPE (purity higher than 99%) was acquired from Sigma-Aldrich (St. Louis, MO, USA) and dissolved in chloroform (Synth, Diadema, Brazil, purity higher than 99%) to prepare a solution with concentration of 0.5 mg/mL. The monolayer subphase contained water purified using a Milli-Q-Plus System (resistivity 18.2 MΩ. cm, pH 5.5). Alamar blue (resazurin) was purchased from Molecular Probes (Invitrogen, Brazil). DMSO and MeOH were obtained from Merck (Brazil). RPMI medium, Hank's balanced salts and phosphate-buffered saline (PBS) were obtained from Sigma (Brazil). Other reagents were purchased from Sigma Aldrich (Brazil). All the experiments were performed at a temperature of 25 ± 1 °C

2.2. Plant material

Leaves of *D. brasiliensis* were collected in Campos do Jordão, São Paulo, SP, in August 2009. A voucher specimen was prepared and compared with that deposited at Herbarium of *Prefeitura Municipal de São Paulo* (PMSP) under number PMSP8984.

2.3. Extraction and isolation

Dried and powdered leaves (896 g) of *D. brasiliensis* were exhaustively extracted using *n*-hexane at room temperature. After concentration under reduced pressure, 29.6 g of *n*-hexane extract were obtained. Part of the crude material (680 mg) was subjected to column chromatography on a silica gel eluted with increasing amounts of EtOAc in *n*-hexane to afford *epi*-polygodial (31 mg, 99% of purity).

Epi-polygodial. Pale yellow oil; ^{1}H NMR ($CDCl_3$, 500 MHz): δ 9.87 (d, J = 2.1 Hz, H-11), 9.42 (s, H-12), 7.08 (dd, J = 5.5 and 2.2 Hz, H-7), 3.28 (m, H-9), 0.95 (s, H-14), 0.98 (s, H-15), 0.93 (s, H-13). ^{13}C NMR ($CDCl_3$, 125 MHz): 202.3 (C-11), 192.8 (C-12), 153.5 (C-7), 137.4 (C-8), 58.5 (C-9), 44.2 (C-5), 42.0 (C-3), 37.7 (C-10), 37.1 (C-1), 32.9 (C-13), 32.7 (C-4), 25.5 (C-6), 21.9 (C-14), 21.5 (C-15), 18.4 (C-2). LREIMS *m/z* (rel. int.): 234 (18), 230 (25), 215 (12), 203 (47), 191 (29), 177 (27), 161 (23), 148 (31), 133 (25), 119 (29), 105 (46), 91 (82), 77 (62), 69 (67), 55 (60), 41 (100).

2.4. Parasites and mammalian cell maintenance

Trypomastigotes of *T. cruzi* (Y strain) were maintained in Rhesus monkey kidney cells (LLC-MK2-ATCC CCL 7), cultivated in RPMI-1640 medium supplemented with 2% FBS at 37 °C in a 5% CO_2-humidified incubator. Macrophages were collected from the peritoneal cavity of BALB/c mice by washing them with RPMI-1640 medium supplemented with 10% FBS and were maintained at 37 °C in a 5% CO_2-humidified incubator. The murine conjunctive cells (NCTC clone 929, ATCC) and LLC-MK2 were maintained in RPMI-1640 supplemented with 10% FBS at 37 °C in a humidified atmosphere containing 5% CO_2.

2.5. Anti-trypomastigote activity

Free trypomastigotes obtained from LLC-MK2 cultures were counted in a Neubauer hemocytometer and seeded at 1×10^6 microplates. To determine the 50% inhibitory concentration (IC_{50}) values, *epi*-poligodial and benznidazole (standard drug) were dissolved in DMSO, diluted in RPMI-1640 medium and maintained for 24 h at 37 °C in a 5% CO_2 humidified incubator. The viability of the trypomastigotes was verified by resazurin (Alamar Blue®) assay using a microplate reader (FilterMax F5 Multi-Mode Microplate Reader) with excitation and emission wavelengths of 540 nm and 595 nm, respectively [14].

2.6. Cytotoxicity in mammalian cells

NCTC cells-clone L929 (6×10^4 cells/well) were seeded and incubated with the *epi*-polygodial (200–1.56 μM) for 48 h at 37 °C in a 5% CO_2 incubator. The cytotoxic concentration (CC_{50}) was determined by MTT assay. The optical density was determined in FilterMax F5 (Molecular Devices) at 570 nm. The selectivity index (SI) was determined using the following equation: CC_{50} against NCTC cells/IC_{50} against parasites [15].

2.7. Langmuir monolayers

The DPPE solution was spread on the air-water interface of water contained in a Langmuir trough from KSV Instruments (model: mini), and 10 min were waited for evaporation of chloroform. Preliminary tests were carried out with *epi*-polygodial dissolved in chloroform to a concentration of 0.5 mg/mL: its solution was also spread alone at the air-water interface in order to test its surface activity. For mixed monolayers containing DPPE and *epi*-polygodial (5% in mol), the phospholipid and the bioactive compound were co-spread on the air-water interface.

The monolayers were compressed with an interface compression rate of 5 $Å^2$ molecule^{-1} min^{-1} to the collapse of the film. Stability curves were carried out pre-compressing the monolayers up to 30 mN/m and registering the surface pressure variation with time with the barriers stopped. For PM-IRRAS (polarization modulation infrared reflection-absorption spectroscopy) and BAM (Brewster Angle Microscopy) studies, the monolayers were also compressed up to 30 mN/m, and maintained constant by slowing moving the barriers back and forth to compensate the surface pressure variations. When it is no longer necessary to trigger the barriers to keep the surface pressure of 30 mN/m constant, the monolayer is considered stable and the infrared spectrum is then taken.

The PM-IRRAS measurements were then taken using a KSV PMI 550 instrument (KSV Instruments, Ltd., Helsinki, Finland) at a fixed incidence angle of 80° and the BAM images using a mini-BAM Microscopy from KSV-Nima.

Each data (tensiometric data, image or spectrum) shown in this paper was repeated at least three times for checking the reproducibility and only representative curves, images or spectra are shown.

3. Results and discussion

The ^{1}H NMR spectrum showed two peaks assigned to aldehydes at δ 9.87 (d, J = 2.1 Hz, H-11) and at 9.42 (s, H-12) as well as a peak attributed to a conjugated olefinic hydrogen at δ 7.08 (dd, J = 5.5 and 2.2 Hz, H-3). These signals associated to the singlets at δ 0.95 (CH_3-14), 0.98 (CH_3-15), and 0.93 (CH_3-13) suggested the occurrence of an isomer of sesquiterpene polygodial, previously isolated from *D. brasiliensis* [3]. ^{13}C NMR spectrum showed 15 signals being two assigned to carbonyl carbons at δ 202.3 (C-11) and 192.8 (C-12), two attributed to olefinic carbons at δ 153.5 (C-7) and 137.4 (C-8) as well as three referring to methyl carbons at δ 21.9 (C-14), 21.5 (C-15), and 32.9 (C-13). Finally, LREIMS spectrum (70 eV) showed a $[M]^+$ ion peak at *m/z* 234, consistent with molecular formula $C_{15}H_{22}O_2$. The comparison of obtained NMR and LREIMS data with those reported in the literature [4], confirmed the structure of *epi*-poligodial as shown in Fig. 1.

The IC_{50} (50% inhibitory concentration) and CC_{50} (50% cytotoxic concentration) obtained for *epi*-polygodial and for the positive control benznidazole against the trypomastigote form of *T. cruzi* and to NCTC cells, respectively, are presented in Table 1. As could be observed, *epi*-polygodial showed an IC_{50} value of 5.0 μM, and benznidazole IC_{50} value of 16.4 μM. The obtained results indicated also a reduced toxicity to *epi*-poliogial (CC_{50} > 200 μM) with a SI > 40. Considering the need for new hit compounds with reduced toxicity for Chagas disease [16] and the potential of polygodial as new scaffolds, *epi*-polygodial could

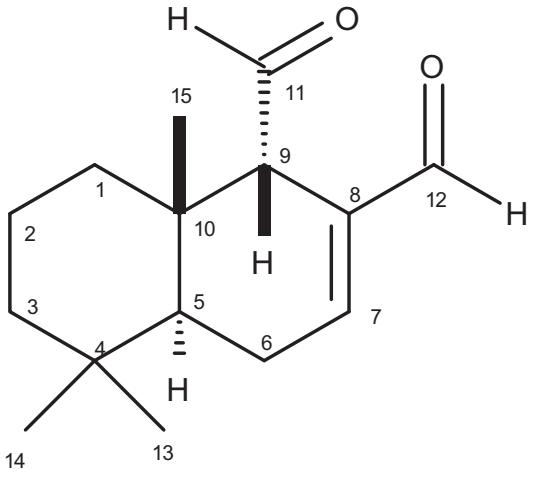

Fig. 1. Structure of sesquiterpene *epi*-poligodial, isolated from *D. brasiliensis*.

Table 1
Anti-*T. cruzi* (trypomastigote forms) and mammalian cytotoxicity (NCTC cells) for *epi*-polygodial and benznidazole.

	IC_{50}/μM (95% CI)	CC_{50}/μM (95% CI)	SI
	Trypomastigote	*NCTC*	
Epi-polygodial	5.01 (4.51–5.56)	> 200	> 40.0
Benznidazole	16.40 (13.31–19.59)	> 200	> 12.2

SI: Selectivity index = CC_{50} of NCTC/IC_{50} of trypomastigotes; 95% CI – 95% confidence interval.

represent a future candidate for optimization studies in drug design against *T. cruzi*.

Based on these results, it is interesting to start investigating the molecular action mechanism of this drug against protozoans. Many microbicidal drugs act disturbing the cellular membrane, or passing through it to attain the cytoplasm [17] or simply destroying it [18]. Consequently, the understanding of the physical chemical effects when these drugs interact with lipid interfaces is fundamental. Also, lipid-drug interactions are interesting for process involving drug delivery by using liposomes.

When *epi*-polygodial spread alone on the air-water interface, as a surface active compound, the compression of the interface provokes the increase of the surface pressure monotonically up to 22 mN/m. Further compression leads to a lower rate of increase of surface pressure probably caused by molecular accommodation at the interface. However, it attains a relatively low area per molecule attained (about 8 $Å^2$) in relation to its molecular dimensions suggests aggregation of the compound, formation of multilayers or desorption towards the aqueous subphase, indicating that *epi*-polygodial does not assemble films at the air-water interface as a stable monomolecular film.

Fig. 2 shows the surface pressure-area ($\pi - A$) isotherm for DPPE, alone or mixed with *epi*-polygodial. This lipid was chosen because PE-based lipids are frequently found in *T. cruzi* cellular membranes [11]. DPPE presents a typical curve, with a liquid-condensed state appearing with compression, which resembles to that reported in the literature [19]. At lower DPPE molecular densities, the isotherm is shifted to higher areas because of the presence of *epi*-polygodial, indicating the incorporation of the compound. For surface pressures higher than 25 mN/m, the isotherm for the mixed film turns shifted to lower areas in relation to the isotherm for pure DPPE. This suggests the expelling of the drug from the monolayer with compression, but it is also possible that this compound is not completely expelled from the interface vicinities since *epi*-polygodial may interact with the polar heads of DPPE in the shear layer just below the lipid-water interface. Such interaction

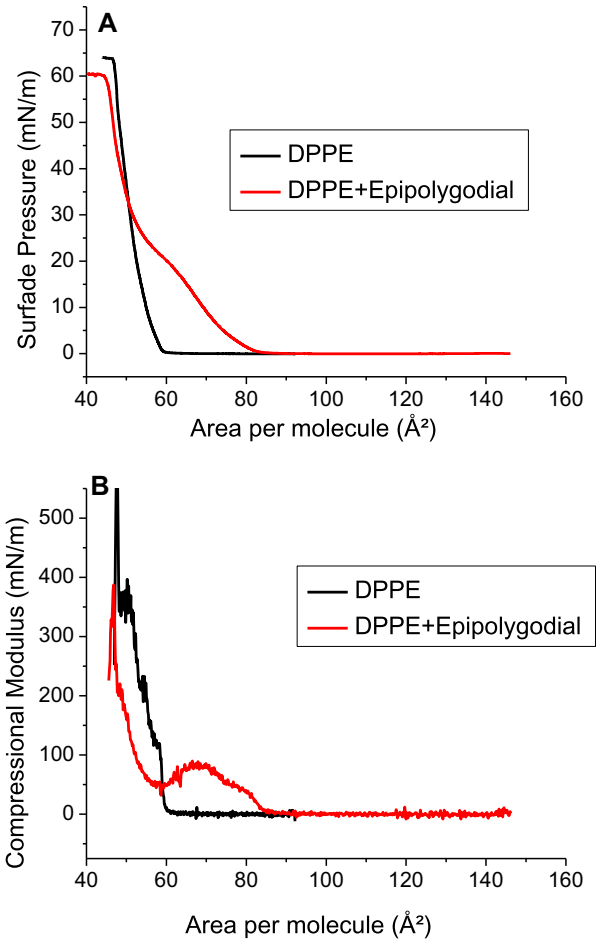

Fig. 2. Surface pressure-area (A) and Compressional modulus-area (B) for DPPE, alone or mixed with *epi*-polygodial 5% in mol, as indicated in the inset. Area per molecule is calculated only for DPPE for better comparison.

also would lead to the shift of the isotherm to lower areas due to monolayer condensation. This fact may occur owing to the minimization of the repulsion between adjacent lipid polar heads, which may stabilize the interface due to intermolecular interactions between *epi*-polygodial and the polar head of DPPE.

Compressional modulus, defined as $-A(\partial\pi/\partial A)_T$, can be calculated directly from the π-A isotherm, as shown in Fig. 2B. In molecular areas lower than 62 $Å^2$, it is clear a sudden increased in the compressional modulus values for the pure DPPE monolayer suggesting a progressively compacted monolayer. For the mixed monolayer, we observe in molecular areas between 85 and 70 $Å^2$, approximately, a decrease in the modulus from 100 to 60 mN/m, roughly. With further compression, the modulus also increases sharply. The local decrease in the values of the compressional modulus may be associated to the mechanism of expelling of *epi*-polygodial from a position between adjacent lipid chains towards the polar heads of DPPE, i.e. at the shear layer of the lipid-water interface. In other words, the energy given to the monolayer by the compression, instead of resulting of an elastic increase of surface pressure, is employed for this molecular rearrangement at the interface, with the film presenting, therefore, viscoelastic features.

It is also important to note appearance of a phase transition induced by *epi*-polygodial, which is visible in the isotherm as a "pseudo"-plateau at 60 $Å^2$ (25 mN/m) and can be depicted in the compressibility modulus dependency as a minimum. Such a behavior prove that this transition is of first order and can be attributed to molecular rearrangements of *epi*-poligodial along the lipid molecules at the air-water interface when subjected to compression.

Fig. 3 shows the so-called stability curves. The monolayers were

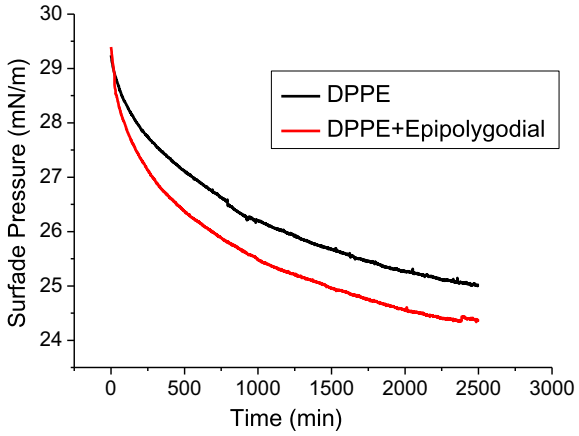

Fig. 3. Surface pressure-time curves for DPPE, alone or mixed with *epi*-polygodial 5% in mol, as indicated in the inset.

compressed to 30 mN/m and barriers stopped in order to follow the spontaneous variation of surface pressure to reach equilibrium. This value of surface pressure was particularly chosen because it represents the lateral pressure of cellular membranes [20].

As the compression mechanism should be too fast for the equilibrium rearrangement to take place, the surface pressure tends to decrease when the monolayer is compressed to higher surface pressures due to mechanisms of molecular relaxation. For pure DPPE, the surface pressure decreases from 30 mN/m to 25 mN/m in 40 min, and for the mixed monolayer, the decrease leads to values as low as 24 mN/m. Considering the resolution of the sensor (below 0.1 mN/m), this difference is significant and indicates a destabilization of the monolayer caused by the presence of *epi*-polygodial, allowing for molecular rearrangements to relax thermodynamically the monolayer.

PM-IRRAS spectra for the monolayers at 30 mN/m are shown in Fig. 4. The bands centered at 2851 and 2917 cm^{-1} for pure DPPE are attributed to symmetric and antisymmetric stretches for CH_2, respectively. At the same time, the symmetric and antisymmetric C—H stretching of the terminal $-CH_3$ groups appear at 2877 and 2964 cm^{-1}, respectively. The frequencies of the CH_2 stretching absorption bands are sensitive to the conformational changes of the chains [21–24] and when the chains are highly ordered (all-*trans* conformation), narrow absorption bands appear around CH_2. For the mixed monolayer, the antisymmetric band is shifted to 2929 cm^{-1}, indicating an increase of the order of the monolayer [25]. This corroborates with the π-A isotherms, in which at 30 mN/m, the isotherm is shifted to lower areas, being suggested an interaction of *epi*-polygodial with the polar heads of DPPE.

Panel B shows that the C=O stretch band, centered at 1735 cm^{-1}, is relatively little affected with the presence of *epi*-polygodial. However, the bands attributed to phosphate (1096 and 1220 cm^{-1}) are clearly altered, suggesting an interaction of the drug with this group. The set of bands that appear at 1500 and 1700 cm^{-1} are mainly attributed to interfacial waters, which is an artefact resulted from the difference of reflectivity of the interface covered and uncovered by the monolayer [26]. The band centered at 1453 cm^{-1} is attributed to CH_2 bending vibrations.

Fig. 5 shows the images with BAM for the monolayers. DPPE, clearly, does not present contrast of phases up to 30 mN/m since forms a compacted monolayer. For the mixed monolayer, however, at 20 mN/m, small aggregates are observed as a consequence of the film expansion. With compression, *epi*-polygodial is rearranged at the interface towards the polar heads of the lipid, and at 30 mN/m, the monolayer became again homogeneous.

With these results, we can note that *epi*-polygodial disturb monolayers formed with DPPE, expanding the film at high molecular areas,

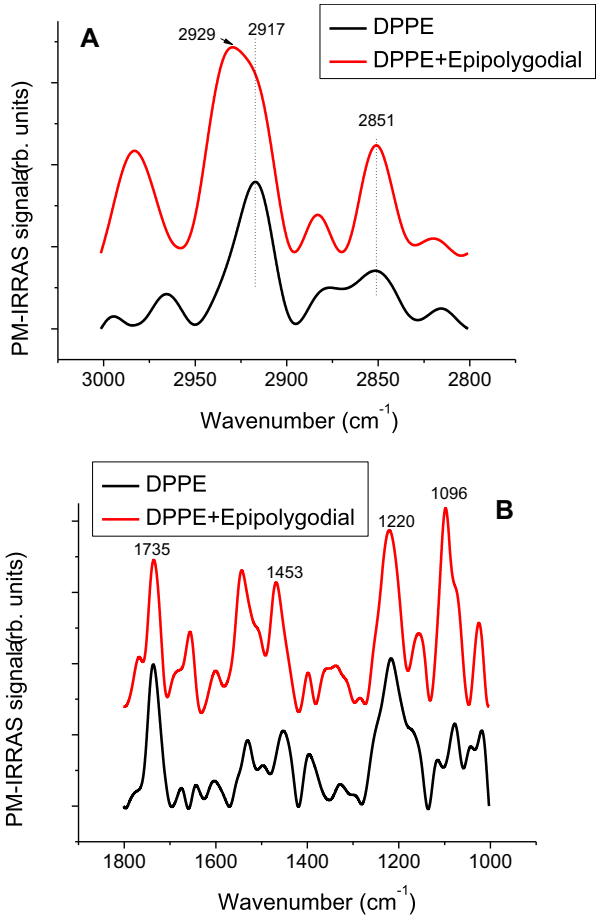

Fig. 4. PM-IRRAS for DPPE monolayers, alone or mixed with *epi*-polygodial 5% in mol, as indicated in the inset. Surface pressure of 30 mN/m.

but condensing it at low molecular areas. This process could be confirmed with data of infrared spectroscopy and BAM, in which the vibrational spectra and the morphology are affected upon incorporation of the compound.

Although the monolayer results do not justify directly the anti-trypanosomal activity of *epi*-polyglodial, it can help understand how this drug can interact with lipid/water biological interfaces (such as cell membranes) in the course of its biological activity. More accurate information can be given with further work involving more complex systems such as unsaturated lipids, membrane proteins, and mixtures involving two or more lipids.

4. Conclusions

In this work we report the isolation and anti-*T. cruzi* activity of sesquiterpene *epi*-polygodial from leaves of *D. brasiliensis*. *Trypanosoma cruzi* trypomastigotes were susceptible to treatment using *epi*-polygodial (IC_{50} value of 5.01 μM) about 3-fold more effective than the positive control benznidazole (IC_{50} value of 16.4 μM). Regarding the cytotoxicity, both compounds displayed CC_{50} values higher than 200 μM and SI values of > 40 and > 12.2 to *epi*-polygodial and benznidazole, respectively. The obtained results suggested that *epi*-polygodial could be considered a candidate molecule for further investigations, including *in vivo* assays against *T. cruzi*. This compound affected remarkably the physical chemical properties of protozoal cell membrane models, represented by DPPE monolayers. *Epi*-polygodial expanded DPPE monolayers in higher lipid molecular areas, but condensed them at low molecular densities, suggesting a preferential interaction with the polar heads of the lipid. Such mechanism of action

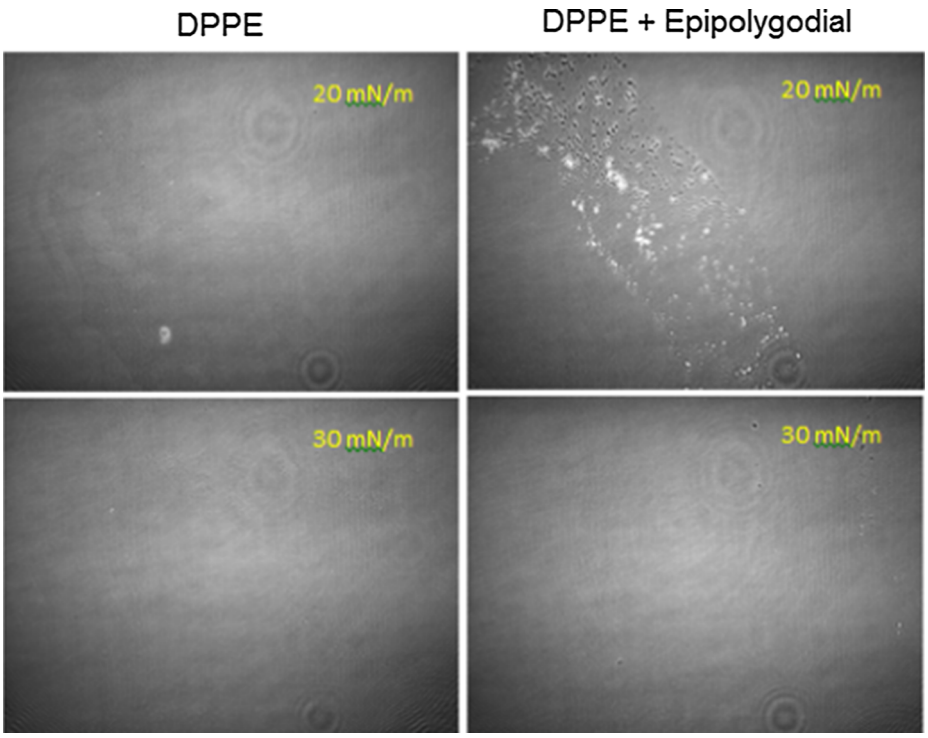

Fig. 5. BAM images for DPPE monolayers, alone or mixed with *epi*-polygodial 5% in mol, as indicated in the inset (dimensions: 4000 × 3600 μm).

affects directly the rheological and morphological properties of the monolayer, leading to altered profiles in the compressional modulus isotherm as well in the pattern of BAM images, with aggregates in the mixed monolayers that disappear with compression. Also PM-IRRAS corroborated this information pointing to a decrease of the *trans*-gauche transitions for the methylene groups. These results point therefore that the interaction of *epi*-polygodial with lipids at the air-water interface alters the thermodynamic, viscoelastic, structural and morphological properties of the biomimetic surface, pointing to a more condensed monolayer due to a preferential interaction with the lipid-water shear layer. We expect that these results have a substantial impact on the comprehension on the molecular mechanism of action of this compound in biological surfaces. The possible biological implications of these findings may be related to the effects caused by incorporating *epi*-polygodial into the Langmuir monolayer, especially at surface pressure values that approximate natural cellular membrane pressures.

Acknowledgments

FAPESP (2018/07885-1, 2015/23446-0, 2015/23403-9 and 2013/14262-7) and CNPq (400896/2016-8). We thank CAPES for scholarships for GEGG, TRM, KSG, and TACS. We also thank CNPq for the grant award to AGT, JHGL and LC.

Appendix A. Supplementary material

Supplementary data to this article can be found online at https://doi.org/10.1016/j.bioorg.2018.11.048.

References

[1] H. Anke, O. Sterner, Comparison of the antimicrobial and cytotoxic activities of twenty unsaturated sesquiterpene dialdehydes from plants and mushroom, Planta Med. 57 (1991) 346–346.
[2] F.M. da Cunha, T.S. Fröde, G.L. Mendes, A. Malheiros, V. Cechinel Filho, R.A. Yunes, J.B. Calixto, Additional evidence for the anti-inflammatory and anti-allergic properties of the sesquiterpene polygodial, Life Sci. 70 (2001) 159–169.
[3] D.S. Corrêa, A.G. Tempone, J.Q. Reimão, N.N. Taniwaki, P.P. Romoff, O.A. Fávero, P. Sartorelli, M.C. Mecchi, J.H.G. Lago, Anti-leishmanial and anti-trypanosomal potential of polygodial isolated from stem barks of *Drimys brasiliensis* Miers (Winteraceae), Parasitol. Res. 109 (2011) 231–236.
[4] B. Rodríguez, N. Zapata, P. Medina, E. Viñuela, A complete ^{1}H and ^{13}C NMR data assignment for four drimane sesquiterpenoids isolated from *Drimys winterii*, Magn. Reson. Chem. 43 (2005) 82–84.
[5] B. Pecoul, C. Batista, E. Stobbaerts, I. Ribeiro, R. Vilasanjuan, J. Gascon, M.J. Pinazo, S. Moriana, S. Gold, A. Pereiro, M. Navarro, F. Torrico, M.E. Bottazzi, P.J. Hotez, The BENEFIT trial: where do we go from here? PLoS Negl. Trop. Dis. 10 (2016) e0004343.
[6] I. Langmuir, The constitution and fundamental properties of solids and liquids. II. Liquids, J. Am. Chem. Soc. 39 (1917) 1848–1906.
[7] B. Brockman, Lipid monolayers: why use half a membrane to characterize protein-membrane interactions? Curr. Oppin. Struct. Biol. 9 (1999) 438–443.
[8] T.M. Nobre, F.J. Pavinatto, L. Caseli, L.A. Barros-Timmons, P. Dynarowicz-Latka, O.N. Oliveira, Interactions of bioactive molecules & nanomaterials with Langmuir monolayers as cell membrane models, Thin Sol. Films 593 (2015) 158–188.
[9] C. Stefaniu, G. Brezesinski, H. Möhwald Langmuir, monolayers as models to study processes at membrane surfaces, Adv. Colloid Interf. Sci. 208 (2014) 197–213.
[10] Juan J. Giner-Casares, Gerald Brezesinski, Helmuth Möhwald, Langmuir monolayers as unique physical models, Curr. Op. Coll. & Int. Sci. 19 (2014) 176–182.
[11] J.F. da Silveira, W. Colli, Chemical composition of the plasma membrane from epimastigote forms of *Trypanosoma cruzi*, Biochim. Biophys. Acta 644 (1981) 341–350.
[12] P. Wydro, K. Witkowska, The interactions between phosphatidylglycerol and phosphatidylethanolamines in model bacterial membranes: the effect of the acyl chain length and saturation, Colloid Surf. B: Biointerf. 72 (2009) 32–39.
[13] K. Hoc-Wydro, J. Kapusta, A. Jagoda, P. Wydro, P. Dynarowicz-Latka, The influence of phospholipid structure on the interactions with nystatin, a polyene antifungal antibiotic - a Langmuir monolayer study, Chem. Phys. Lipids 150 (2007) 125–135.
[14] J.Q. Reimão, A.E. Migotto, M.H. Kossuga, R.G. Berlinck, A.G. Tempone, Antiprotozoan activity of Brazilian marine cnidarian extracts and of a modified steroid from the octocoral *Carijoa riisei*, Parasitol. Res. 103 (2008) 1445–1450.
[15] S.S. Grecco, T.A. Costa-Silva, G. Jerz, F.S. de Sousa, V.S. Londero, M.K. Galuppo, M.L. Lima, B.J. Neves, C.H. Andrade, A.G. Tempone, J.H.G. Lago, Neolignans from leaves of *Nectandra leucantha* (Lauraceae) display *in vitro* antitrypanosomal activity via plasma membrane and mitochondrial damages, Chem. Biol. Interact. 277 (2017) 55–61.
[16] A. Rea, A.G. Tempone, E.G. Pinto, E. Mesquita, L.G. Rodrigues, P. Silva, J.H.G. Lago, Sartorelli Soulamarin isolated from *Calophyllum brasiliense* (Clusiaceae) induces plasma membrane permeabilization of *Trypanosoma cruzi* and mitochondrial dysfunction, PLoS Negl. Trop. Dis. 5 7 (12) (2013) e2556.
[17] C.A. Bell, C.C. Dykstra, N.A. Naiman, M. Cory, T.A. Fairley, R.R. Tidwell, Structure-activity studies of dicationically substituted bis-benzimidazoles against giardia-lamblia - correlation of antigiardial activity with DNA-binding affinity and Giardial Topoisomerase II inhibition, Antimicrob. Agents Chemother. 37 (1993) 2668–2673.
[18] W.C. Wimley, Describing the mechanism of antimicrobial peptide action with the interfacial activity model, ACS Chem. Biol. 15 (2010) 905–917.

[19] D. Gidalevitz, Y. Ishitsuka, A.S. Muresan, O. Konovalov, A.J. Waring, R.I. Lehrer, K.Y. Lee, Interaction of antimicrobial peptide protegrin with biomembranes, Proc. Natl. Acad. Sci. USA 27 (2003) 6302–6307.
[20] A. Blume, A comparative study of the phase transitions of phospholipid bilayers and monolayers, Biochim. Biophys. Acta 557 (1979) 32–34.
[21] Y.Q. Li, H. Ishida, Concentration-dependent conformation of alkyl tail in the nanoconfined space: hexadecylamine in the silicate galleries, Langmuir 19 (2003) 2479–2484.
[22] N.V. Venkataraman, S. Vasudevan, Conformation of methylene chains in an intercalated surfactant bilayer, J. Phys. Chem. B. 105 (2001) 1805–1812.
[23] R. Mendelsohn, J.W. Brauner, A. Gericke, External infrared reflection absorption spectrometry of monolayer films at the air-water interface, Annu. Rev. Phys. Chem. 46 (1995) 305–334.
[24] S. Barman, N.V. Venkataraman, S. Vasudevan, R. Seshadri, Phase Transitions in the Anchored Organic Bilayers of Long-Chain Alkylammonium Lead Iodides ($C_nH_{2n}+1NH_3$)2PbI_4; n = 12, 16, 18, J. Phys. Chem. B. 107 (2003) 1875–1883.
[25] F.R. Rana, S. Widayati, B.W. Gregory, R.A. Dluhy, Metastability in monolayer films transferred onto solid substrates by the Langmuir-Blodgett method: IR evidence for transfer-induced phase, Trans. Appl. Spectrosc. 48 (1994) 1196–1203.
[26] J. Saccani, S. Castano, F. Beaurain, M. Laguerre, B. Desbat, Stabilization of phospholipid multilayers at the air-water interface by compression beyond the collapse: a BAM PM-IRRAS, and molecular dynamics study, Langmuir 20 (2004) 9190–9197.